![jove logo] Journal of Visualized Experiments

Video Article

Focal Macropatch Recordings of Synaptic Currents from the *Drosophila* Larval Neuromuscular Junction

Alexander Vasin[1], Maria Bykhovskaia[1,2]

[1]Department of Neurology, School of Medicine, Wayne State University

[2]Department of Anatomy and Cell Biology, School of Medicine, Wayne State University

Correspondence to: Maria Bykhovskaia at mbykhovs@med.wayne.edu

Abstract

Drosophila neuromuscular junction (NMJ) is an excellent model system to study glutamatergic synaptic transmission. We describe the technique of focal macropatch recordings of synaptic currents from visualized boutons at the *Drosophila* larval NMJ. This technique requires customized fabrication of recording micropipettes, as well as a compound microscope equipped with a high magnification, long-distance water immersion objective, differential interference contrast (DIC) optics, and a fluorescent attachment. The recording electrode is positioned on the top of a selected synaptic bouton visualized with DIC optics, epi-fluorescence, or both. The advantage of this technique is that it allows monitoring the synaptic activity of a limited number of sites of release. The recording electrode has a diameter of several microns, and the release sites positioned outside of the electrode rim do not significantly affect the recorded currents. The recorded synaptic currents have fast kinetics and can be readily resolved. These advantages are especially important for the studies of mutant fly lines with enhanced spontaneous or asynchronous synaptic activity.

Video Link

The video component of this article can be found at https://www.jove.com/video/56493/

Introduction

Drosophila is an excellent model system to study the molecular mechanisms controlling synaptic transmission. The neuromuscular system in *Drosophila* is glutamatergic, and therefore the *Drosophila* neuromuscular junction (NMJ) can be used to study the conserved features of glutamatergic release. Since Jan and Jan's study[1], the third instar larvae has been broadly used to study evoked and spontaneous synaptic transmission by monitoring excitatory junction potentials (EJPs) or currents (EJCs). EJPs are commonly recorded intracellularly with a sharp glass micro-electrode, and they reflect the activity of the entire NMJ, including all the boutons making synapses at the given muscle fiber.

In contrast, the activity of a limited number of the sites of release can be recorded focally by positioning a micropipette tip near neuronal terminals or synaptic varicosities. This technique was originally employed by Katz and Miledi[2], and focal extracellular recordings have been successfully employed at several NMJ preparations, including frog[3,4,5], mouse[6,7,8], crustacean[9,10,11,12,13,14,15,16], and *Drosophila*[17,18,19,20,21,22,23]. This approach was further developed by Dudel, who optimized macropatch recoding electrodes[24,25]. In Dudel's implementation, this technique closely matched the loose-patch-clamp method[26].

The *Drosophila* larval NMJ has clearly defined synaptic boutons, and transgenic lines with genetically encoded neuronal fluorescent tags (see **Table of Materials**) are readily available. These advantages enabled us to record EJCs and mEJCs from a selected synaptic bouton[20,21,22]. Here, we describe this technique in detail.

Protocol

1. Fabrication of Recording Electrodes

1. **Pulling the glass electrodes**
    1. Use the following protocol for the microelectrode puller (see **Table of Materials**):
        1. Line 1: Heat 510 Pull - Velocity 30 Time 250; Line 2: Heat 490 Pull - Velocity 30 Time 250.
        NOTE: Time units correspond to 0.5 ms per unit; the other units are relative. The value of the heat should be adjusted for every filament after the ramp test is performed.

2. Use a microscope (35x magnification) to ensure that the inner diameter of the pulled electrode is in the range of 7 - 10 μm (**Figure 1A**). Store the capillaries in tightly closed containers to prevent dust accumulation.

2. **Fire polishing**
   1. Fire polish capillaries (80 - 90% of the maximum heat value for 1 - 2 s) using a micro-forge (see **Table of Materials**). Ensure the final inner diameter of the polished electrode is 5 μm (**Figure 1A**)[27].

3. **Bending**
   NOTE: Two bends are made in order to position the electrode on the top of the muscle under a high magnification objective.
   1. Use the apparatus shown in **Figure 1B**. Fix the electrode in the manipulator and position the tip over the filament, not touching it.
   2. Set heat value to 60 - 70% of the maximum and press the pedal of the micro-forge for 1 - 2 s (see **Table of Materials**) to heat the filament. Use an L-shaped needle to gently pull down the tip of the electrode (**Figure 1B** enlarged). Make the bend at approximately 90° (**Figure 1C**).
   3. Hold the electrode over the flame of the torch by hand using forceps and make the second bend at a distance of 7 - 10 mm from the first bend and at an angle of approximately 120° (**Figure 1C**).
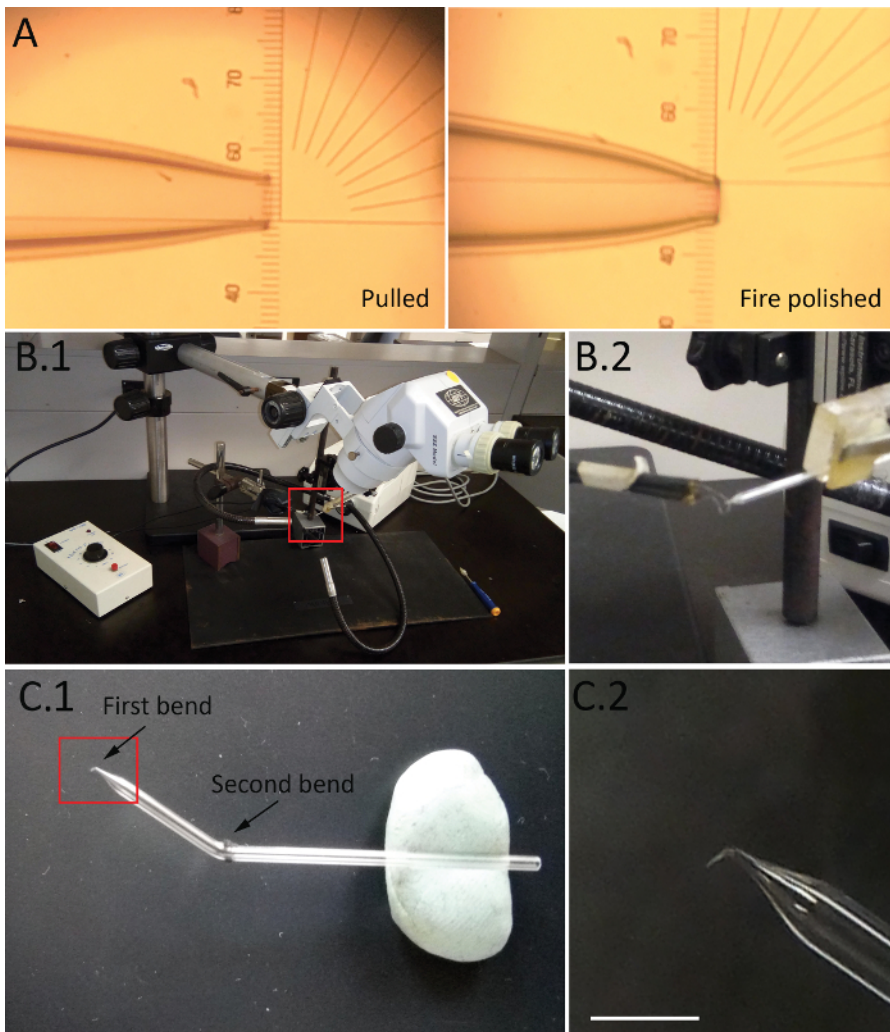

Figure 1. Final steps of micropipette fabrication. (**A**) Electrode tips after pulling and fire polishing. (**B.1**) The setup for tip bending. (**B.2**) The boxed area is shown enlarged on the right. The electrode and the filament are fixed so that the electrode tip is positioned slightly above the wire and not touching. (**C.1**) The recording electrode. (**C.2**) The boxed area is shown enlarged on the right. The first bend has an angle of approximately 90°, and the distance between the first bend and the tip of the electrode is approximately 1 mm. Scale bar = 3 mm. Please click here to view a larger version of this figure.

2. Additional Preparatory Steps

1. Prepare heamolymph-like (HL3) solution (in mM): 70 NaCl, 5 KCl, 20 $MgCl_2$, 10 $NaHCO_3$, 5 trehalose, 115 sucrose, 5 HEPES, and 1 mM $CaCl_2$; adjust the pH to 7.3 - 7.4. Keep the solution in the refrigerator and make it fresh every week.
2. Make stimulation pipets the same way as recording glass pipets, except there is no need to bend them.

NOTE: The preparation of stimulation electrodes is described in detail in [28] and [27]. The final diameter after fire polishing should be in the range of 5 - 7 µm.

3. Insert a stimulation pipette in a microelectrode holder connected to a syringe.
4. Manufacture dissection plates from small petri dishes (35 x 10 mm) coated with silicone rubber epoxy (see **Table of Materials**) as described in [28].
    NOTE: Silicone rubber should be completely hardened before use.
5. Pick a wandering third-instar larvae and dissect it as described in[27,28,29,30].
    NOTE: To visualize boutons, use the fly strain CD8-GFP (see **Table of Materials**)
    1. Using forceps (see **Table of Materials**), pick the 3rd instar larvae from a vial.
    2. Pin the larvae, placing the first pin posterior and another pin anterior (close to mouth hooks).
    3. Add HL3 solution.
    4. Make a cut using spring scissors (see **Table of Materials**) all the way from the top pin to the bottom one on the dorsal side of the larvae.
    5. Pin the larvae fillet, placing 2 additional pins on the left and right sides of the larvae.
    6. Remove the guts and tracheas using forceps.
    7. Cut the nerves just outside the ventral nerve cord using spring scissors.
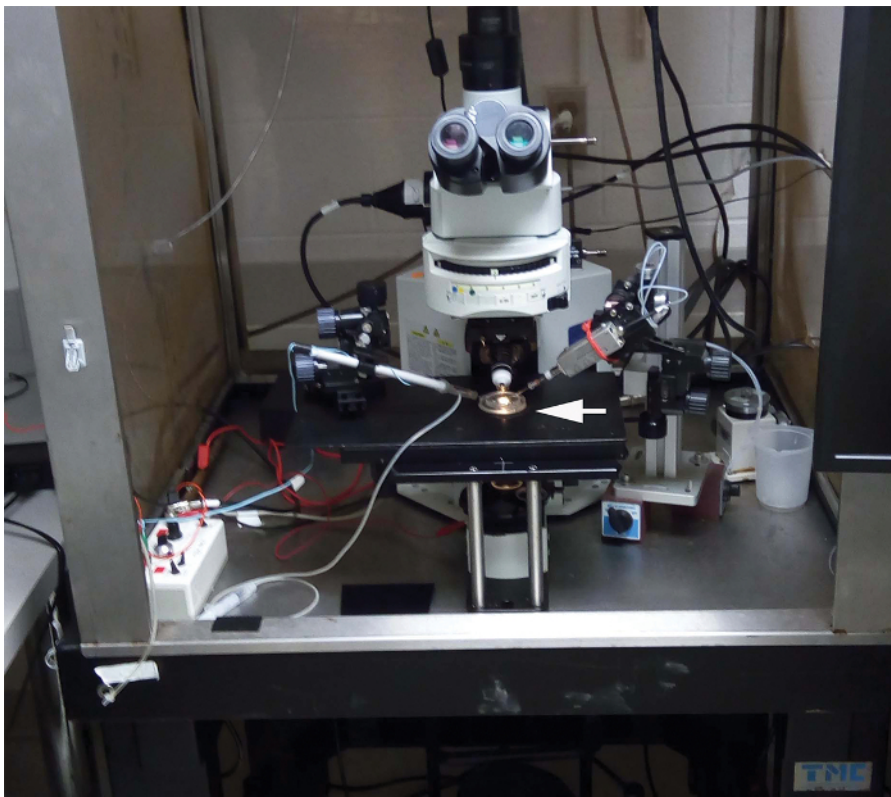
3. Electrical recordings of EJCs

Figure 2. The recording setup. The sample NMJ pinned to the silicon coated petri dish (arrow) is positioned over the movable stage of the upright compound microscope equipped with epifluorescence capabilities, a high magnification objective, and two micromanipulators. The microscope is stationed on an anti-vibration table. Please click here to view a larger version of this figure.

1. **Recording**
    1. Place the petri dish with the preparation on the microscope stage (**Figure 2**). Insert the reference electrode in the bath.
    2. Fill the recording electrode with HL3 solution. Under the 10x objective (see **Table of Materials**), immerse the electrode into the bath and place it over muscles 6 and 7 of the abdominal segments 2, 3, or 4 using the micromanipulator (see **Table of Materials**) (**Figure 3 A.1 and A.2**).
    3. Switch the objective to 60x (see **Table of Materials**). Focus on the area of interest using either epi-fluorescence or DIC optics. Place the tip of the electrode on top of synaptic bouton (**Figure 3 B.1-3**).
    4. Press the electrode very gently onto the muscle. Excessive pressure may damage the NMJ or induce an increase in spontaneous synaptic activity. Make sure the tip of the electrode is not clogged- if it is, replace it.
    5. Switch on the amplifier, A/D board, and the computer.
    6. Choose the voltage clamp mode on the amplifier.
    7. Start acquisition software and choose the 'gap-free' mode.
    8. Observe the appearance of mEJCs on the computer screen.
    9. Ensure that the amplitude of the mEJCs is in the range of 0.2 - 0.7 nA.

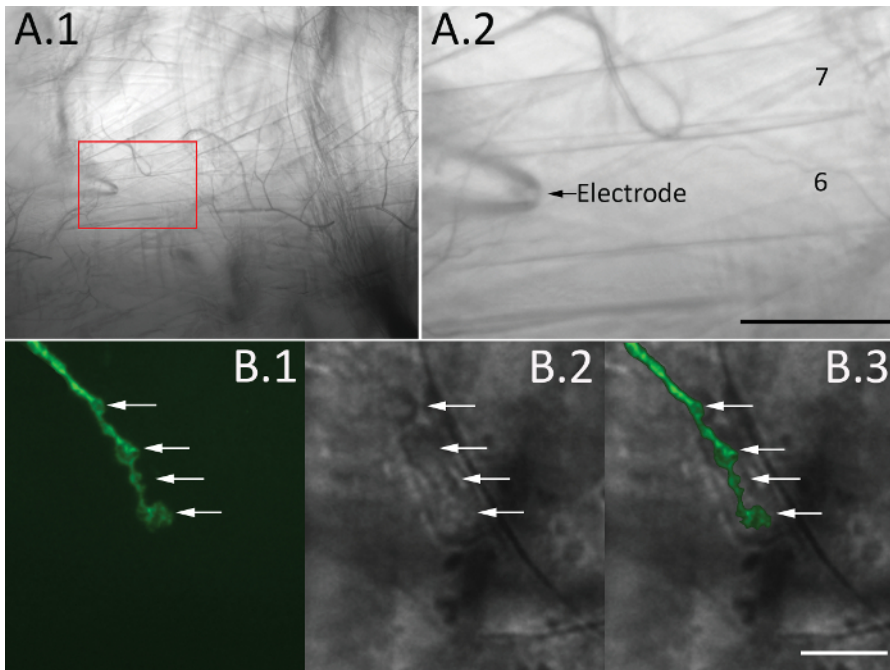NOTE: Smaller EJCs indicate that the recording electrode has defects or that it is not positioned properly.

Figure 3. Visualization of synaptic boutons. (**A**) A brightfield image of a hemi-segment under 10x magnification (**A.1**) and the enlarged boxed area showing muscles 6 and 7 (**A.2**, the arrow marks the recording electrode). Scale bar = 50 μm. (**B**) Synaptic boutons are visualized in a *Drosophila* line with a genetically encoded neuronal marker (CD8-GFP) using epi-fluorescence imaging (**B.1**) or DIC optics (**B.2**). Images are taken with the 60x objective and the filter cube for GFP imaging (see **Table of Materials**). Synaptic boutons are marked with arrows, and an overlay of fluorescent and DIC images is shown in **B.3**. Scale bar = 10 μm. Please click here to view a larger version of this figure.

2. **Stimulation**
    1. Using a micromanipulator, under a visual control, place the stimulation electrode near the axon innervating abdominal segments 2 - 4.
    2. Apply negative pressure by pulling the piston of the syringe connected to the electrode holder, so that the axon is pulled inside of the electrode (**Figure 2**).
    3. Turn on the stimulator. Turn the knob on the isolation unit (see **Table of Materials**) to set a zero current, and then gently increase it, until EJCs appear (or until the threshold is reached).
    4. Perform the stimulation in a suprathreshold regime, with the stimulation current increased approximately twice, compared to the threshold for the observation of EJCs.
    NOTE: In our experience, such stimulation intensity is optimal to avoid action potential failures and action potential firing. For example, if EJCs appear at the stimulation current of 0.2 mA, use a current of 0.4 mA throughout the experiment.

3. **Seal resistance**
    1. Measure the seal resistance of the recording macropatch electrode by turning the electrode resistance switch of the amplifier to "seal test" position. Observe that the value of seal resistance in GΩ will be displayed in the "current" window.
    2. Make sure the seal resistance is in the range of 0.5 - 2 MΩ. Values out of this range indicate that the electrode is not properly polished or not properly positioned.
    3. Monitor the seal resistance throughout the recording, making sure it remains constant throughout the experiment.

4. Analysis

1. Analyze recordings employing customized software for analysis (see **Table of Materials**).
    NOTE: Our lab uses in-house software Quantan[31], which is customized for the detection of EJCs and mEJCs recorded focally (**Figure 4**). This software includes a Gaussian digital filter and allows the detection of quantal peaks in overlapping multi-quantal events (**Figure 4A**). Other approaches are described in[17].
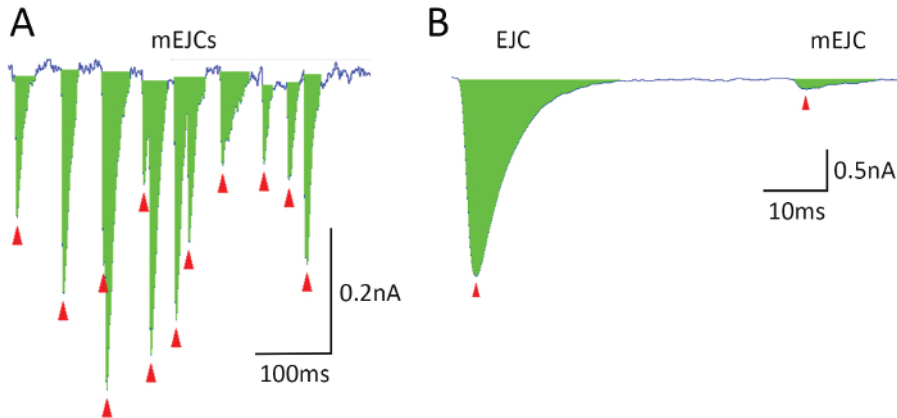
Figure 4. Quantal analysis. Detection of mEJCs (**A**) and EJCs (**B**) by Quantan software. The event area is marked in green, and peaks are marked by red arrowheads. Please click here to view a larger version of this figure.

Representative Results

Focal macropatch recordings enable monitoring synaptic activity from selected synaptic boutons (**Figure 5**). When the electrode is positioned on the top of a synaptic bouton (**Figure 5A**, site 1), the recorded mEJCs (**Figure 5C**, site 1) have a amplitudes significantly exceeding the noise level and sharp rising phases (at a sub-millisecond range). When the recording electrode is moved away from the synaptic bouton by several microns (**Figure 5A**, site 2), the amplitudes of recorded mEJCs decline almost to the noise level (**Figure 5B**, site 2). The recorded EJCs can barely be distinguished from the noise and they have prolonged rising phases (**Figure 5C**, site 2 versus site 1).

The limited number of release sites contributing to recorded EJCs and mEJCs, as well as rapid kinetics of synaptic currents recorded focally, enables accurate detection of release events in mutants with elevated synaptic activity. This can be clearly illustrated by recordings of mEJCs from complexin null mutant (**Figure 6A**). Spontaneous activity is drastically elevated in this mutant[32], and therefore mEJPs recorded intracellularly overlap and cannot be clearly distinguished from each other (**Figure 6B**), while focal recordings[22] enable accurate detection of spontaneous release events (**Figure 4A**).
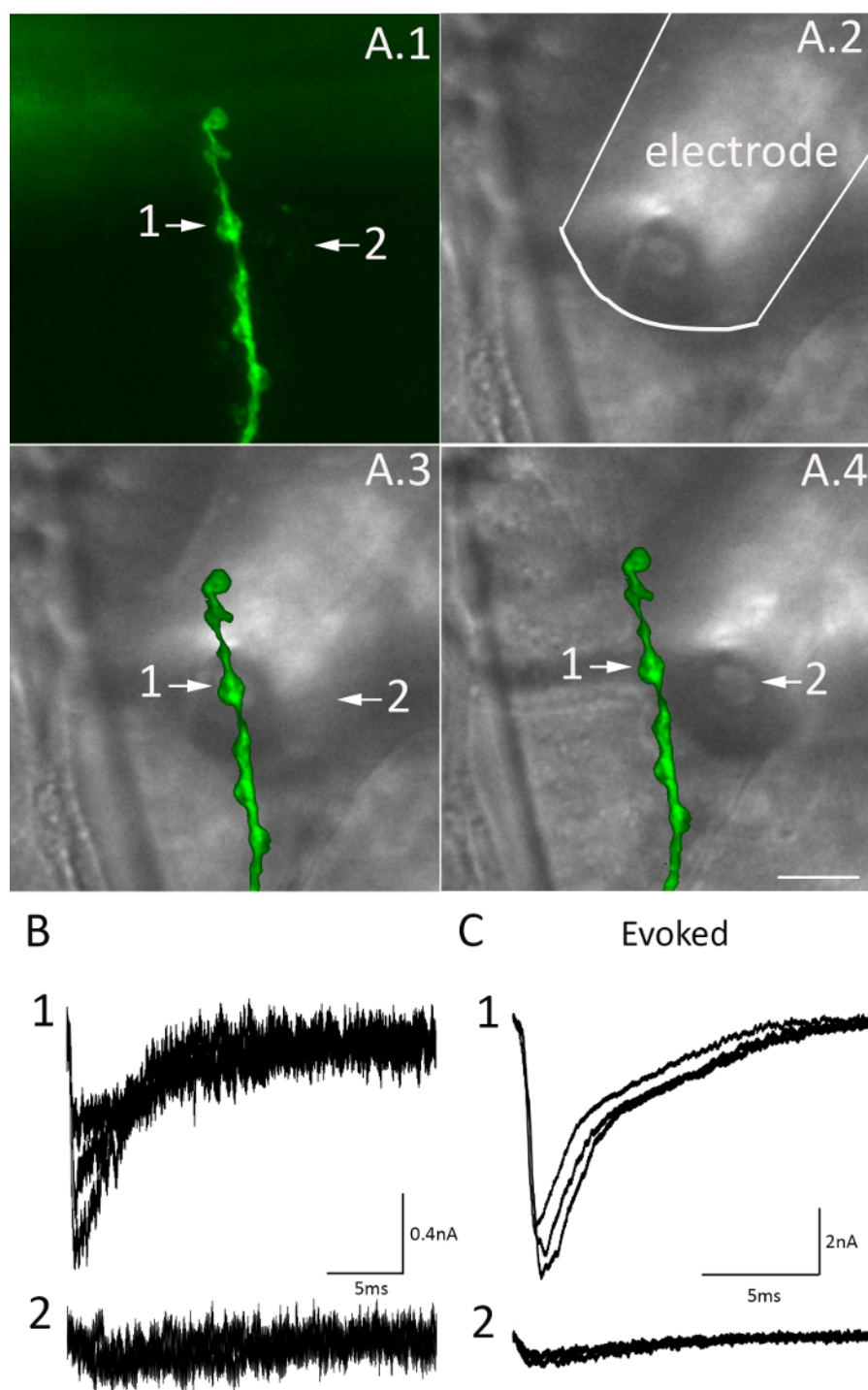
Figure 5. Recordings of EJCs and mEJCs from a selected bouton. (**A**) Placing the electrode over a selected bouton (site 1) and moving it away from the bouton (site 2). The images show the CD8-GFP tagged NMJ visualized with epi-fluorescence (**A.1**), recording electrode over the muscle fiber (**A.2**), and overlays (**A.3, A.4**), with the electrode positioned over site 1 (**A.3**) or site 2 (**A.4**). Scale bar = 10 μm. (**B**) mEJCs recorded from the bouton (site 1) are clearly distinguished from the recording noise and have rapid rising phases. In contrast, mEJCs recorded from site 2 cannot be reliably distinguished from the recording noise, their amplitudes are reduced several-fold, and they have a slower time-course. (**C**) The Amplitudes of EJCs recorded from the bouton (site 1) exceed by many-fold the amplitudes of EJCs recorded from site 2, and they also have more rapid kinetics. Please click here to view a larger version of this figure.
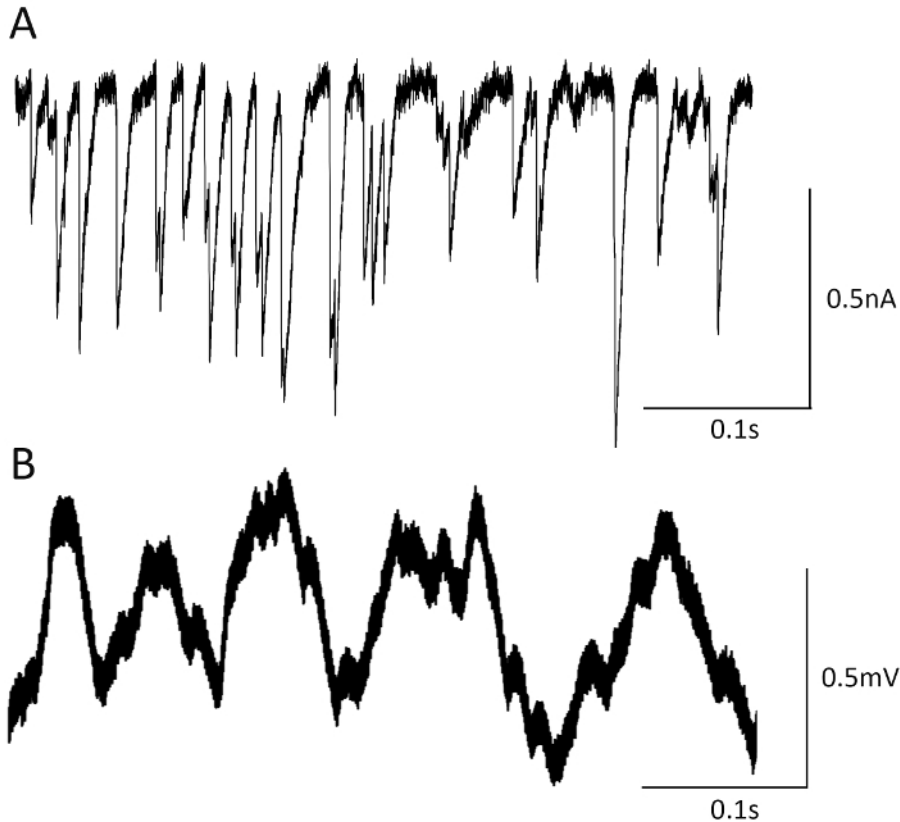
Figure 6. Focal macropatch versus intracellular recordings. Focal recordings enable accurate detection of mEJCs in the complexin null mutant (**A**), while intracellular recordings (**B**) from this mutant exhibit release events that overlap and cannot be reliably detected. Please click here to view a larger version of this figure.

Discussion

Drosophila represents an advantageous model organism to study synaptic transmission. Several recording configurations have been used at the larval NMJ, including intracellular recordings of synaptic potentials, recordings of synaptic currents with two electrode voltage clamp[33,34], and focal macropatch recordings of synaptic currents described here. The latter technique allows the precise quantification of synaptic transmission at visualized boutons.

The success of the described protocol critically depends on the ability to clearly visualize the area of interest and to customize the preparation of recording electrodes. Thus, quality DIC optics, a high magnification water immersion objective with a long working distance, and customized equipment for fire polishing and bending of recording electrodes are critically important.

The advantage of this approach is that it allows monitoring the activity of a few synapses that are positioned under the recording electrode. It should be noted, however, boutons positioned near the rim of the electrode may also contribute to recorded activity. It is critical, therefore, that the position of the electrode, as well as the seal resistance, does not change in the course of the experiment.

The ability to monitor activity of a single bouton can be potentially combined with recent imaging technologies. For example, optical detection of activity at individual active zones[35] can be combined with focal recordings of EJCs and mEJC, and this could couple the spatial resolution of optical detection with temporal resolution of electrical recordings.

Disclosures

The authors have nothing to disclose.

Acknowledgements

References

1. Jan, L. Y., & Jan, Y. N. Properties of the larval neuromuscular junction in Drosophila melanogaster. *J Physiol.* **262** (1), 189-214 (1976).

2. Katz, B., & Miledi, R. The effect of temperature on the synaptic delay at the neuromuscular junction. *J Physiol.* **181** (3), 656-670 (1965).

3. Macleod, G. T., Gan, J., & Bennett, M. R. Vesicle-associated proteins and quantal release at single active zones of amphibian (Bufo marinus) motor-nerve terminals. *J Neurophysiol.* **82** (3), 1133-1146 (1999).

4. Macleod, G. T., Farnell, L., Gibson, W. G., & Bennett, M. R. Quantal secretion and nerve-terminal cable properties at neuromuscular junctions in an amphibian (Bufo marinus). *J Neurophysiol.* **81** (3), 1135-1146 (1999).

5. Zefirov, A., Benish, T., Fatkullin, N., Cheranov, S., & Khazipov, R. Localization of active zones. *Nature.* **376** (6539), 393-394 (1995).

6. Macleod, G. T., Lavidis, N. A., & Bennett, M. R. Calcium dependence of quantal secretion from visualized sympathetic nerve varicosities on the mouse vas deferens. *J Physiol.* **480** (Pt 1) 61-70 (1994).

7. Samigullin, D., Bill, C. A., Coleman, W. L., & Bykhovskaia, M. Regulation of transmitter release by synapsin II in mouse motor terminals. *J Physiol.* **561** (Pt 1), 149-158 (2004).

8. Coleman, W. L., & Bykhovskaia, M. Rab3a-mediated vesicle recruitment regulates short-term plasticity at the mouse diaphragm synapse. *Mol Cell Neurosci.* **41** (2), 286-296 (2009).

9. Atwood, H. L., Parnas, H., Parnas, I., & Wojtowicz, J. M. Quantal currents evoked by graded intracellular depolarization of crayfish motor axon terminals. *J Physiol.* **383** 587-599 (1987).

10. Parnas, H., Dudel, J., & Parnas, I. Neurotransmitter release and its facilitation in crayfish. I. Saturation kinetics of release, and of entry and removal of calcium. *Pflugers Arch.* **393** (1), 1-14 (1982).

11. Wojtowicz, J. M., Marin, L., & Atwood, H. L. Activity-induced changes in synaptic release sites at the crayfish neuromuscular junction. *J Neurosci.* **14** (6), 3688-3703 (1994).

12. Zucker, R. S. Crayfish neuromuscular facilitation activated by constant presynaptic action potentials and depolarizing pulses. *J Physiol.* **241** (1), 69-89 (1974).

13. Zucker, R. S. Changes in the statistics of transmitter release during facilitation. *J Physiol.* **229** (3), 787-810 (1973).

14. Worden, M. K., Bykhovskaia, M., & Hackett, J. T. Facilitation at the lobster neuromuscular junction: a stimulus-dependent mobilization model. *J Neurophysiol.* **78** (1), 417-428 (1997).

15. Bykhovskaia, M., Hackett, J. T., & Worden, M. K. Asynchrony of quantal events in evoked multiquantal responses indicates presynaptic quantal interaction. *J Neurophysiol.* **81** (5), 2234-2242 (1999).

16. Bykhovskaia, M., Polagaeva, E., & Hackett, J. T. Mechnisms underlying different facilitation forms at the lobster neuromuscular synapse. *Brain Res.* **1019** (1-2), 10-21 (2004).

17. Cooper, R. L., Stewart, B. A., Wojtowicz, J. M., Wang, S., & Atwood, H. L. Quantal measurement and analysis methods compared for crayfish and Drosophila neuromuscular junctions, and rat hippocampus. *J Neurosci Methods.* **61** (1-2), 67-78 (1995).

18. Stewart, B. A., Atwood, H. L., Renger, J. J., Wang, J., & Wu, C. F. Improved stability of Drosophila larval neuromuscular preparations in haemolymph-like physiological solutions. *J Comp Physiol A.* **175** (2), 179-191 (1994).

19. Pawlu, C., DiAntonio, A., & Heckmann, M. Postfusional control of quantal current shape. *Neuron.* **42** (4), 607-618 (2004).

20. Akbergenova, Y., & Bykhovskaia, M. Synapsin maintains the reserve vesicle pool and spatial segregation of the recycling pool in Drosophila presynaptic boutons. *Brain Res.* **1178** 52-64 (2007).

21. Akbergenova, Y., & Bykhovskaia, M. Enhancement of the endosomal endocytic pathway increases quantal size. *Mol Cell Neurosci.* **40** (2), 199-206 (2009).

22. Vasin, A., Volfson, D., Littleton, J. T., & Bykhovskaia, M. Interaction of the Complexin Accessory Helix with Synaptobrevin Regulates Spontaneous Fusion. *Biophys J.* **111** (9), 1954-1964 (2016).

23. Wong, K., Karunanithi, S., & Atwood, H. L. Quantal unit populations at the Drosophila larval neuromuscular junction. *J Neurophysiol.* **82** (3), 1497-1511 (1999).

24. Dudel, J. The effect of reduced calcium on quantal unit current and release at the crayfish neuromuscular junction. *Pflugers Arch.* **391** (1), 35-40 (1981).

25. Dudel, J. Contribution of Ca2+ inflow to quantal, phasic transmitter release from nerve terminals of frog muscle. *Pflugers Arch.* **422** (2), 129-142 (1992).

26. Marrero, H. G., & Lemos, J. R. *Loose-Patch-Clamp method.* 2 edn, Humana Press (2007).

27. Wu, W. H., & Cooper, R. L. Physiological recordings of high and low output NMJs on the crayfish leg extensor muscle. *J Vis Exp.* (45) (2010).

28. Verstreken, P., Ohyama, T., & Bellen, H. J. FM 1-43 labeling of synaptic vesicle pools at the Drosophila neuromuscular junction. *Methods Mol Biol.* **440** 349-369 (2008).

29. Brent, J. R., Werner, K. M., & McCabe, B. D. Drosophila larval NMJ dissection. *J Vis Exp.* (24) (2009).

30. Imlach, W., & McCabe, B. D. Electrophysiological methods for recording synaptic potentials from the NMJ of Drosophila larvae. *J Vis Exp.* (24) (2009).

31. Bykhovskaia, M. Making quantal analysis more convenient, fast, and accurate: user-friendly software QUANTAN. *J Neurosci Methods.* **168** (2), 500-513 (2008).

32. Huntwork, S., & Littleton, J. T. A complexin fusion clamp regulates spontaneous neurotransmitter release and synaptic growth. *Nat Neurosci.* **10** (10), 1235-1237 (2007).

33. Zhong, Y., & Wu, C. F. Altered synaptic plasticity in Drosophila memory mutants with a defective cyclic AMP cascade. *Science.* **251** (4990), 198-201 (1991).

34. Delgado, R., Maureira, C., Oliva, C., Kidokoro, Y., & Labarca, P. Size of vesicle pools, rates of mobilization, and recycling at neuromuscular synapses of a Drosophila mutant, shibire. *Neuron.* **28** (3), 941-953 (2000).

35. Melom, J. E., Akbergenova, Y., Gavornik, J. P., & Littleton, J. T. Spontaneous and evoked release are independently regulated at individual active zones. *J Neurosci.* **33** (44), 17253-17263 (2013).